

Synthesis, Spectroscopic, and Photophysical Properties of an Asymmetrically Substituted 2,5-Diarylidene Cyclopentanone Dye: (2E,5E)-2-(benzofuran-2-ylmethylene)-5-((E)-3-(4-(dimethylamino)phenyl)allylidene)cyclopentanone

A Major Qualifying Project Report

Submitted to the Faculty of

WORCESTER POLYTECHNIC INSTITUTE

In partial fulfillment of the requirements for the

Degree of Bachelor of Science

By:

Maxwell A. Kuhns

April 29, 2010

Approved by:

Prof. Robert E. Connors, Ph.D.
Project Advisor

Table of Contents

Abstract.....	3
Acknowledgments	4
List of Figures.....	5
List of Tables	6
Introduction.....	7
Experimental.....	10
Results and Discussion	20
Conclusions	32
References	33
Appendices	34

Abstract

This work extends an interest in the spectroscopic and photophysical properties of symmetrically substituted 2,5-diarylidene cyclopentanones to asymmetrically substituted 2,5-diarylidene cyclopentanone dyes. Attention is given to (2E,5E)-2-(benzofuran-2-ylmethylene)-5-((E)-3-(4-(dimethylamino)phenyl)allylidene)cyclopentanone (ASBZ2). This compound was synthesized via a two-step reaction; the first step involved running a DIMCARB-catalyzed reaction of cyclopentanone with 2-benzofurancarboxaldehyde to form the benzofuran monoarylidene cycloadduct (asbf), while the second step involved reacting asbf with (E)-4-dimethylaminocinnamaldehyde under base-catalyzed conditions. Spectroscopic and photophysical properties have been measured in a wide variety of non-polar and polar protic and aprotic solvents. Fluorescence quantum yields and fluorescence lifetimes show a strong solvent dependence for the compound; fluorescence quantum yields ranging from 0.035 in ethanol to 0.36 in dichloromethane, and fluorescence lifetimes of those tested from 0.31 ns in n-butanol to 0.74 ns in acetone. First-order radiative and nonradiative decay constants have been calculated from the fluorescence quantum yield and lifetime data. The photophysical properties and spectral data show a correlation against the $E_T(30)$ empirical solvent polarity scale. B3LYP/6-31G(d) geometry optimization and TD-DFT spectral calculations were performed.

Acknowledgments

I would like to acknowledge and thank Professor Robert Connors of advising me during the course of my research and for the use of his time, laboratory, and equipment. I would also like to thank Christopher Zoto for the time and knowledge he put in during the course of the project, as well as Meghan Roache who felt like a lab partner for much of the experiments.

List of Figures

Figure 1: Structure of (2E,5E)-2-(benzofuran-2-ylmethylene)-5-((E)-3-(4-(dimethylamino)phenyl)allylidene)cyclopentanone (ASBZ2)	7
Figure 2: Diagram of the Franck-Condon Principle for the solvation of a fluorophore.	8
Figure 3: Reaction mechanism for the synthesis of ASBF	11
Figure 4: ¹ H (top) and ¹³ C (bottom) NMR of ASBF in CDCl ₃	12
Figure 5: Zoomed in ¹ H NMR of ASBF in CDCl ₃	13
Figure 6: Reaction mechanism for the synthesis of ASBZ2.....	14
Figure 7: ¹ H (top) and ¹³ C (bottom) NMR spectra of ASBZ2 in CDCl ₃	15
Figure 8: Zoomed in ¹ H NMR spectra of ASBZ2 in CDCl ₃	16
Figure 9: Absorbance and emission spectra of ASBZ2 in various solvents	22
Figure 10: Plot of maximum absorption and fluorescence wavenumbers (divided by 104) versus the E _T (30) scale in the various solvents.....	24
Figure 11: Plot of maximum absorption and fluorescence wavenumbers (divided by 104) versus the Δf scale in the various solvents.....	25
Figure 12: Plot of fluorescence quantum yield (Φ _f) versus Ū _n of ASBZ2 in solvents of varying polarities.....	27
Figure 14: Computer molecular orbitals of ASBZ2	30
Figure 15: Fluorescence lifetime of ASBZ2 in acetone.....	41

List of Tables

Table 1: Spectroscopic and photophysical characteristics of ASBZ2 in various solvents	23
Table 2: Molecular Orbital Calculations of ASBZ2	30

Introduction

Highly conjugated organic fluorescent dyes have received attention for their wide variety of uses. Of particular interest are the class of 2,5-diarylidene cyclopentanones. These are ketocyanine dyes that have been applied in their use as photosensitizers, solvent polarity probes, fluoroionophores for cation detection and nonlinear optical materials. Research has been reported on C_{2v} -symmetrically unsubstituted diarylidene cyclopentanones, but this research is expanded to asymmetrically substituted diarylidene cyclopentanones.¹ The high degree of π -conjugation, as well as the length of the conjugated arylidene groups give ASBZ2 specific properties as compared to symmetrically substituted dyes and asymmetrically substituted dyes with fewer degrees of π -conjugation. The structure of ASBZ2 is shown in figure 1.

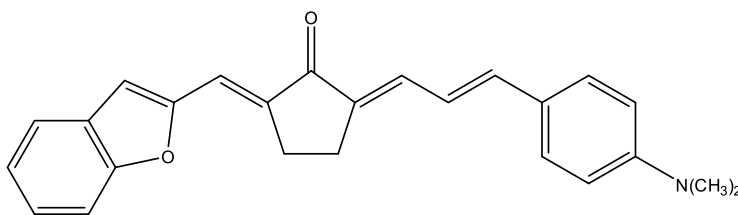


Figure 1: Structure of (2E,5E)-2-(benzofuran-2-ylmethylene)-5-((E)-3-(4-(dimethylamino)phenyl)allylidene)cyclopentanone (ASBZ2)

Applications of conjugated organic fluorophores have also been studied in their use in fluorescent tagging of biological pathways and molecules, as well as HPLC and TLC detection. A more recent application of these fluorescent organic compounds has been as a storage medium in so-called fluorescent multi-layer discs. These discs utilize fluorescent compounds as digital receptors instead of the normal digital reflection used in optical discs. The

fluorescent compounds can be impeded in several layers of the disc, and due to the possible excitation to higher order energy states, capacities of up to terabytes can be achieved on a DVD-sized disc.²

The spectroscopic and photophysical properties of ASBZ2 have been examined in solvents of various polarities, focusing on the solvatochromic properties of the compound. Solvatochromism is the ability of a substance to change color with respect to solvent polarity.³ In absorption and fluorescence spectra a molecule that exhibits solvatochromic properties undergoes either bathochromic (red) or hypsochromic (blue) shifting of the spectra with regard to solvent polarity. Due to the asymmetrical nature of ASBZ2, as well as the electron withdrawing carbonyl group, and the electron donating dimethylamino group, differences in the absorbance and emission characteristics were observed in various solvents as compared to the symmetrically substituted compounds.

The solvatochromic properties of ASBZ2 show a bathochromic shift as the solvent polarity increases. In addition the Stoke's Shift of the compound increases with increasing solvent polarity. This solvatochromic shift causes a color change and a shifting of the absorbance and emission of the compound in more polar solvents. Due to the Franck-Condon principle that molecules do not change position when light is absorbed, the excited state solvent shell is not in equilibrium with the excited state molecule. As the molecule is excited to a higher energy state, a shift in the dipole moment causes a net change in the interaction with the solvent. This varies with the polarity of the solvent.⁴ This is shown in Figure 2. The resulting shift in λ_{max} of the fluorescence relative to λ_{max} in absorption is known as the Stoke's Shift.

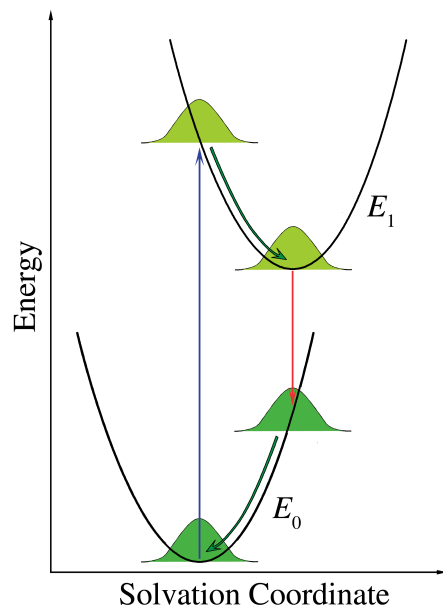


Figure 2: Diagram of the Franck-Condon Principle for the solvation of a fluorophore.

Experimental

1. Synthesis of ASBZ2

The synthesis of ASBZ2 consisted of two steps. The first step involved the synthesis of the intermediate (E)-2-(benzofuran-2-ylmethylene)cyclopentanone (ASBF) via a DIMCARB-catalyzed reaction of cyclopentanone with 2-benzofurancarboxaldehyde. N,N-dimethylammonium-N',N'-dimethylcarbonate or DIMCARB is a dimethylamine carbon dioxide complex that allows for the regioselective (E) addition of the aldehyde to one α -position of the cyclopentanone ring.⁵ In a 25 mL round bottom flask equimolar equivalents (5.0 mmol) of cyclopentanone and the aldehyde were reacted over 27.5 mmol of DIMCARB in 5.5 mL of dichloromethane with continuous stirring at room temperature. The reaction was allowed to run for 90 minutes, and was monitored by TLC co-spotted with the starting material and the desired product. After completion of the reaction, the solvent mixture was removed *in vacuo* and the residue was acidified with 10 mL of 0.5 M H₂SO₄. The product was then extracted with dichloromethane (4x20 mL) and the combined organic layer extracts were dried over anhydrous Na₂SO₄, then filtered. The product was purified by silica gel column chromatography using a gradient approach of hexanes spiked with ethyl acetate over the course of 2 weeks. Purity was confirmed by TLC (showing one spot upon development). Both ¹H and ¹³C NMR in CDCl₃ were used to confirm the structure of ASBF. The hydrogens and carbons in the NMR correlated to that of the molecule. The reaction mechanism for ASBF is shown in figure 3. The ¹H and ¹³C NMR in CDCl₃ can be seen in figure 4.

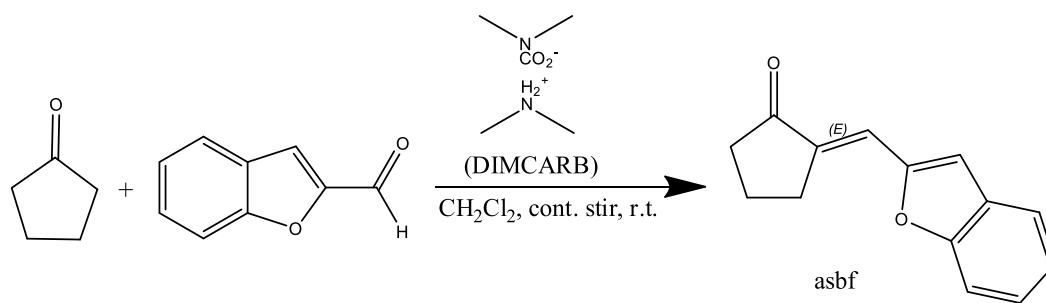
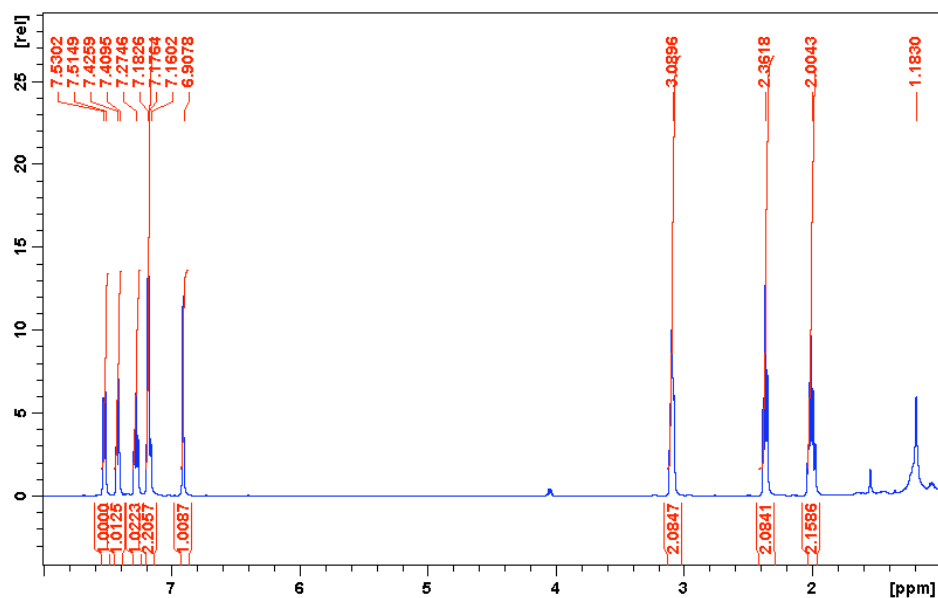


Figure 3: Reaction mechanism for the synthesis of ASBF



VR:

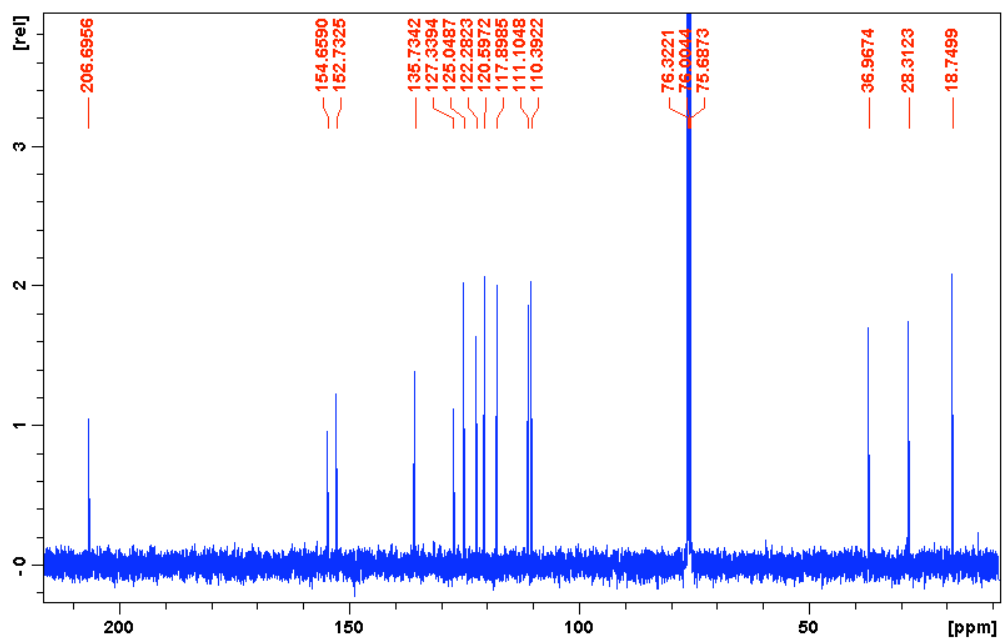


Figure 4: ^1H (top) and ^{13}C (bottom) NMR of ASBF in CDCl_3 . ^1H NMR: δ (ppm)= 7.53–7.51 (d,1H), 7.42–7.41 (d,1H), 7.27 (t,1H), 7.18–7.16 (m,2H), 6.9 (s, 1H), 3.09 (t,2H), 2.36 (t,2H), 2.00 (p,2H). ^{13}C NMR δ (ppm)= 206.7, 154.7, 152.7, 135.7, 127.3, 125.0, 122.3, 120.6, 117.9, 111.1, 110.4, 37.0, 28.3, 18.7

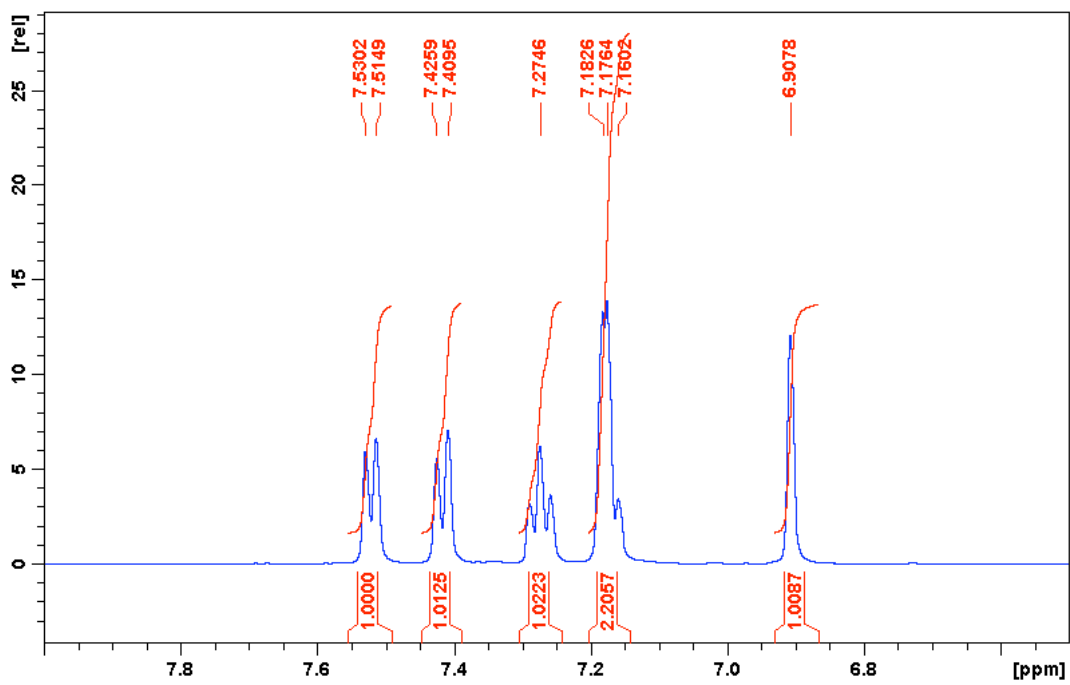
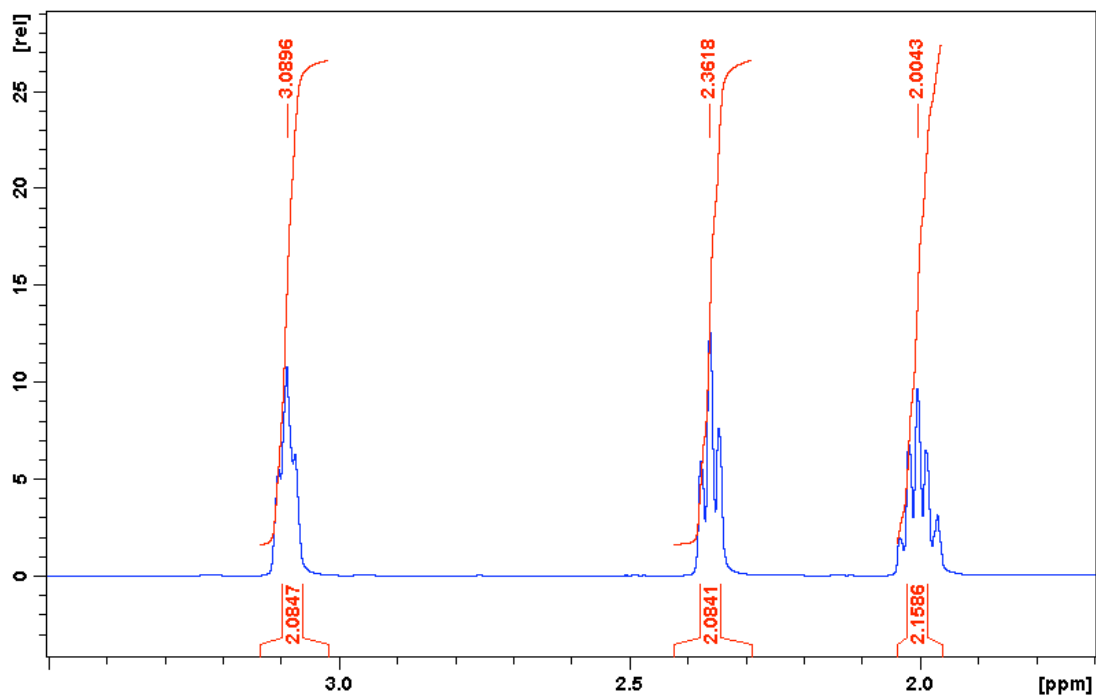


Figure 5: Zoomed in ¹H NMR of ASBF in CDCl₃.

The second step in the synthesis consisted of running an intermolecular base-catalyzed crossed aldol condensation reaction of ASBF with (E)-4-dimethylaminocinnamaldehyde (figure DD). 0.35 g (1.65 mmol) of ASBF were added to 100 mL of ethanol in a clean 250 mL Erlenmeyer flask. Approximately 50 more mL of ethanol was added to completely dissolve the solute. After all the solid had dissolved, 1.0 mL of 2.5% NaOH catalyst was added drop-wise. The solution was allowed to stir for 10 minutes. After 10 minutes equimolar amount of (E)-4-dimethylaminocinnamaldehyde (0.29 g) was carefully added to the solution. Due to the photoreactivity of the compound, the flask was wrapped in aluminum foil. The reaction was allowed to continue over night. A blood-red colored precipitate was filtered *in vacuo*. ¹H and ¹³C NMR spectrum using CDCl₃ were taken to test for the product. The product was then rotovaped with silica gel and purified using silica gel column chromatography with hexanes spiked with ethyl acetate over the course of 3 weeks. ¹H and ¹³C NMR spectrum using CDCl₃ were again taken to structurally determine ASBZ2 and purity was confirmed by TLC. The reaction scheme for ASBZ2 is shown in figure 6. The melting point was found to be 200-203 °C. ¹H and ¹³C NMR spectrum using CDCl₃ spectrum are shown in figure 7.

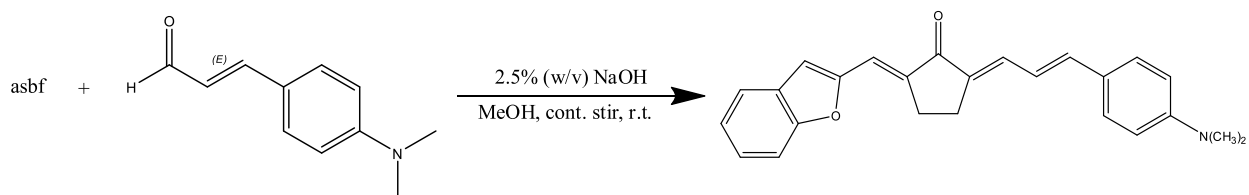


Figure 6: Reaction mechanism for the synthesis of ASBZ2

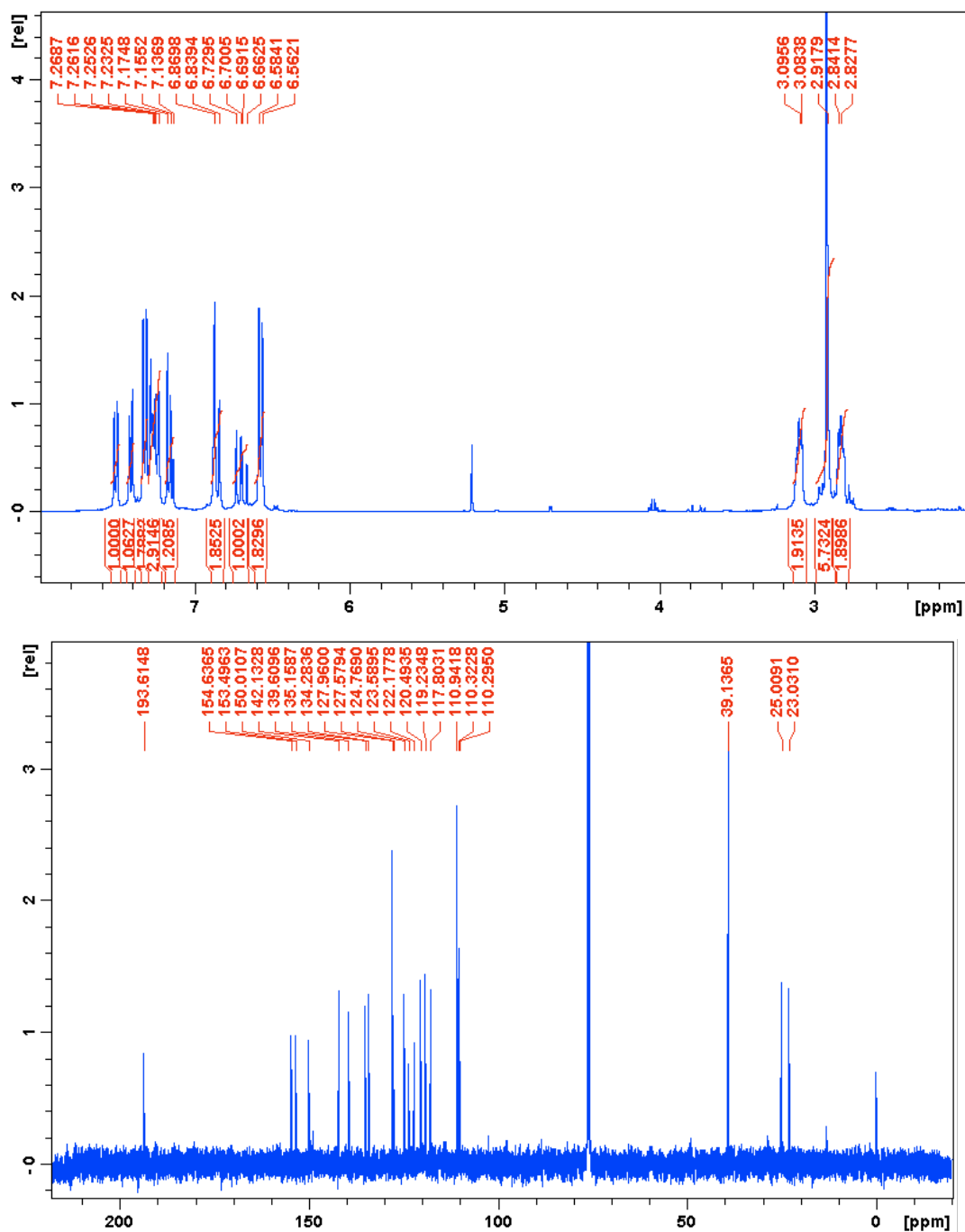


Figure 7: ¹H (top) and ¹³C (bottom) NMR spectra of ASBZ2 in CDCl₃. ¹H NMR: δ (ppm)= 7.52–7.49 (d,1H), 7.42–7.40 (d,1H), 7.33–7.31 (d,2H), 7.28–7.23 (m, 3H), 7.16–7.14 (d,1H), 6.87–6.84 (d,2H), 6.73–6.66 (td,1H), 6.58–6.56 (d,2H), 3.10–3.08 (td,2H), 2.92 (s,6H), 2.84–2.83 (td,2H). ¹³C NMR δ (ppm)= 193.6, 154.6, 153.4, 150.0, 142.1, 139., 135.2, 134.3, 128.0, 127., 124.8, 123.6, 122.2, 120.5, 119.2, 117.8, 110.9, 110.3, 110.3, 39.1, 25.0, 23.0

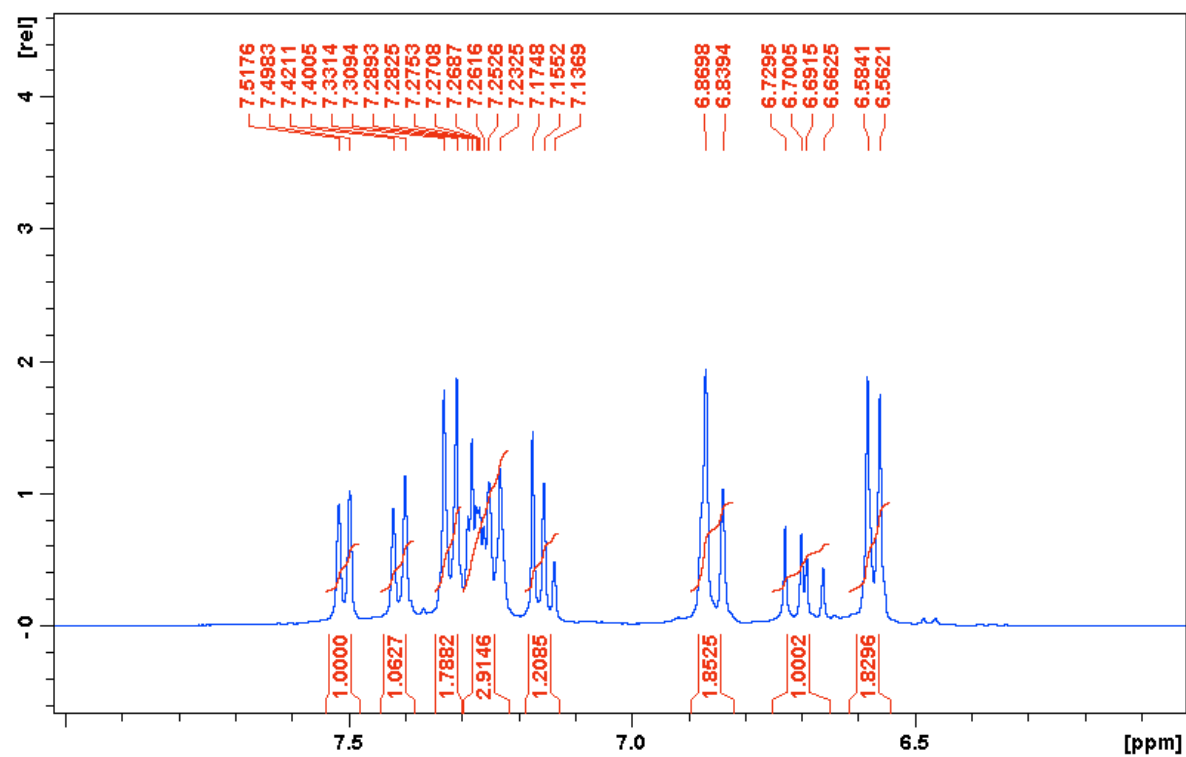
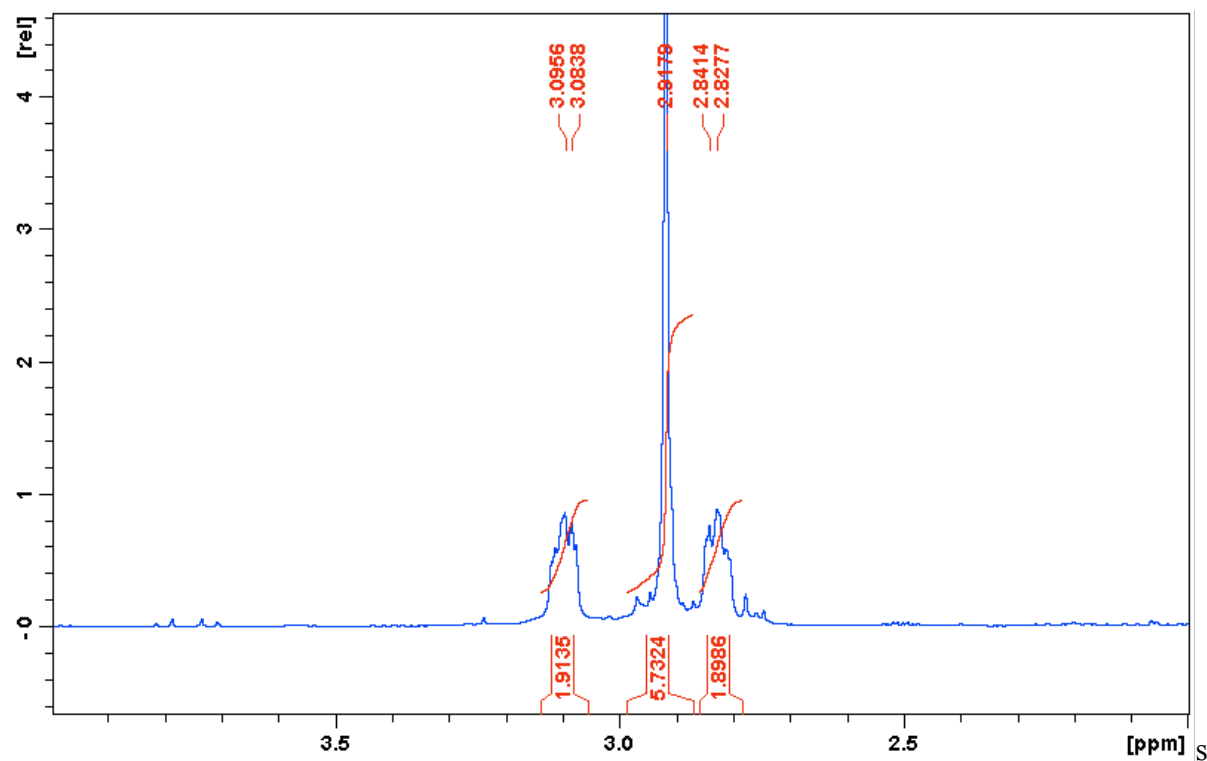


Figure 8: Zoomed in ^1H NMR spectra of ASBZ2 in CDCl_3 .

2. Absorption and Fluorescence Spectra

UV-Vis of ASBZ2 was measured with a Shimadzu UV 2100 Spectrometer having 2 nm band-passes. The fluorescence emission spectra were collected using a Perkin Elmer[®] LS 50B luminescence spectrophotometer equipped with an R928 phototube detector. The NMR spectra were collected using a Bruker[®] AVANCE 400MHz spectrometer.

3. Fluorescence Quantum Yield Determination of ASBZ2

The quantum yield of fluorescence of conjugated organic dyes, such as ASBZ2 is a measure of the efficiency with which absorbed light produces an excited state in the molecule, and can be defined as the ratio of the number of photons emitted to the number of photons absorbed by the fluorochrome. It is represented by the equation:

$$\Phi = \Phi_R \times \frac{Int A_R n^2}{Int_R A n_R^2} \quad \text{Eq. 1}$$

Where Φ is the quantum yield, *Int* are the areas under the corrected emission spectra, *A* is the absorbance at a fixed excitation wavelength, and *n* is the refractive index of the sample. The subscript (*R*) denotes the appropriate values for the reference sample. A solution of fluorescein in 0.1 M NaOH was used as the quantum yield standard. In order to correct the fluorescence emission spectra for instrument response, the literature emission of N,N-dimethylamino-3-nitrobenzene (N,N-DMANB) was compared to the experimental emission spectrum using the LS 50B status.² Scale factors were determined between 12,500 and 22,000 cm⁻¹ at intervals of 50 cm⁻¹.

Absorption was measured using solvents of differing polarities. The solvents used: ethanol, n-propanol, n-butanol, acetonitrile, acetone, dichloromethane (DCM), ethyl acetate, diethyl ether, carbon disulfide (CS₂), tetrahydrofuran (THF), toluene, and n-hexane. Absorbance of a stock solution was gathered at a maximum absorbance of ~0.5. The solution was then diluted tenfold. Both emission and absorbance measurements were performed twice for reproducibility. Corrected emission wavelengths were made using a stock solution of fluorescein in 0.1 N NaOH, which was measured and diluted in the same manner. Correction was applied for instrument response. Wavelengths were exported to Apple Numbers[®] to convert to wavenumbers, and then imported onto MathCad[®] to adjust for the corrected emission spectra. MathCad was used to calculate the area under the corrected fluorescence emission spectra and to compute the fluorescence quantum yields.⁶ Appendix A shows a sample calculation for the fluorescence quantum yield of ASBZ2 in acetone. Grapher[®] was used to create graphs spectral data.

4. Fluorescent Lifetime Determination

The fluorescence lifetime of a compound (τ_f) is defined as the inverse of the sum of the first-order radiative and nonradiative rates of decay:

$$\tau_f = 1 / (k_f + k_{nr}) \quad \text{Eq. 2}$$

Where $k_{nr} = k_{ic} + k_{isc}$. The fluorescence lifetimes (τ_f) of ASBZ2 were measured in the following four solvents: acetone, CS₂, n-butanol, and diethyl ether. Photon Technology International fluorescence lifetime spectrometer equipped with a GL-3300 nitrogen laser and GL-302 dye laser compartments was used for the lifetime measurements. In order to prevent quenching of

the excited state by molecular oxygen, the sample was first degassed with N₂ for at least 5 minutes. The fluorescence decay curves of the analyze were then measured. Felix 32 software was used to analyze the fluorescence decay curves. The fluorescence decay profile of an instrument response function (IRF) was generated at approximately the same maximum intensity as the sample decay; an aqueous non-dairy creamer was used as the IRF. Neutral density filters were used to appropriately adjust the fluorescence intensity of the IRF profile upon generating the fluorescence decay curves as well as the IRF. Fluorescence lifetimes were measured via a curve-fitting procedure, and lifetimes were selected on how well the field-fit curve aligned with the sample decay curve by statistical analysis. Appendix B shows a sample calculation for the fluorescence lifetime determination of ASBZ2 in acetone.

Results and Discussion

1. Introduction

After the synthesis of ASBZ2, the compounds solvatochromic properties were measured with regard to absorbance, fluorescence, fluorescence quantum yields, and fluorescence lifetime decays. These properties were measured in 12 different non-polar, polar aprotic, and polar protic solvents. The solvatochromic properties visually represented themselves by a bathochromic (red) shift in color of the various solvents as polarity increased: when the dark maroon colored ASBZ2 was dissolved the more non-polar solvents showed a yellow to orange color, while the polar aprotic solvents showed a red to maroon color; the polar protic solvents interestingly showed a bright pink color. Maximum absorbance and fluorescence were measured, and quantum yields were calculated from the data. The melting point of ASBZ2 was found to be between 200 and 203 °C.

2. Absorption and Fluorescence Properties

The absorption and fluorescence spectra of 6 solvents varying in polarities is given in figure 9. The spectra show the general trend of the bathochromic shift as solvent polarity increases. This shift occurs in both absorption and emission, however the figure shows that the shift is much greater in emission than in absorbance; the Stoke's shift increases as solvent polarity increases. In addition the spectra broaden as polarity increases. The bathochromic shift and the greater shift in emission can be seen in figures 10 and 11 where fluorescence and absorption wavenumbers are plotted against the solvent polarity function (Δf) and the empirical solvent polarity scale [$E_T(30)$]. These numbers are also listed in Table 1.

The solvent polarity function (Δf) and $E_T(30)$ are empirical values based on literature.

They are dependent on the polarity of the solvent, and the equation for Δf is given³:

$$\Delta f = \frac{\epsilon - 1}{2\epsilon + 1} - \frac{n^2 - 1}{2n^2 - 1} \quad \text{Eq. 3}$$

where ϵ is the dielectric constant and n is the refractive index of the solvent. $E_T(30)$ is based on the solvatochromic charge transfer shift of $E_T(30)$, a betaine dye.³

The shift in the absorbance and fluorescence, as well as the increase in Stoke's Shift are caused by solvatochromic properties between ASBZ2 molecules and the solvent. Since ASBZ2 has an electron withdrawing carbonyl group and an electron donating amino group, the polarity of the solvent affects the difference in dipole moment between the ground and excited state.

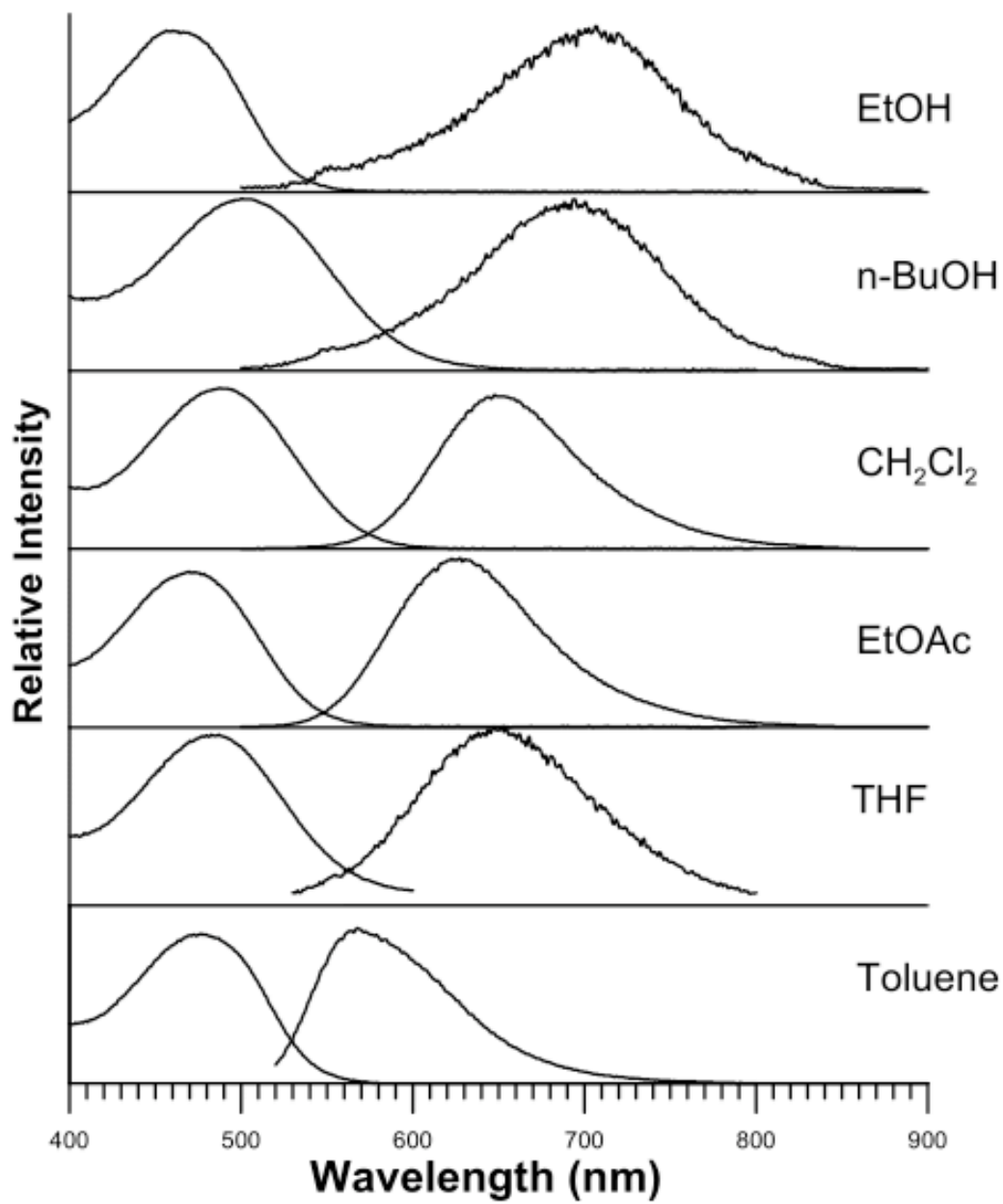


Figure 9: Absorbance and emission spectra of ASBZ2 in various solvents.

Table 1: Spectroscopic and photophysical characteristics of ASBZ2 in various solvents³.

Solvent	$\tilde{\nu}_{fl}$ (cm^{-1})	$\tilde{\nu}_{abs}$ (cm^{-1})	Δf^*	$E_T(30)$ (kcal/mol)	Φ_f	τ_f (ns)	k_f (s^{-1})	k_{nr} (s^{-1})
Ethanol	13571 (737 nm)	20040 (499 nm)	0.2843	51.9	0.035	-	-	-
n-Propanol	13622 (734 nm)	19841 (504 nm)	0.2746	50.7	0.056	-	-	-
n-Butanol	13605 (735 nm)	19960 (501 nm)	0.2642	50.2	0.073	0.3	2.35×10^8	2.99×10^9
Acetonitrile	13588 (736 nm)	20964 (477 nm)	0.3054	45.6	0.091	-	-	-
Acetone	13650 (733 nm)	20921 (478 nm)	0.2843	42.2	0.154	0.7	2.08×10^8	1.14×10^9
DCM	14880 (672 nm)	20492 (488 nm)	0.2171	40.7	0.357	-	-	-
Ethyl Acetate	15135 (661 nm)	21277 (470 nm)	0.1996	38.1	0.28	-	-	-
Diethyl Ether	16520 (605 nm)	21495 (466 nm)	0.1669	34.5	0.165	0.7	2.43×10^8	1.23×10^9
CS ₂	16410 (609 nm)	20450 (489 nm)	-0.0007	32.8	0.127	0.5	2.40×10^8	1.65×10^9
THF	14098 (709 nm)	20534 (487 nm)	0.2104	37.4	0.059	-	-	-
Toluene	16792 (596 nm)	20964 (477 nm)	0.0131	33.9	0.129	-	-	-
n-Hexane	18722 (534 nm)	23697 (422 nm)	-0.0004	-	-	-	-	-

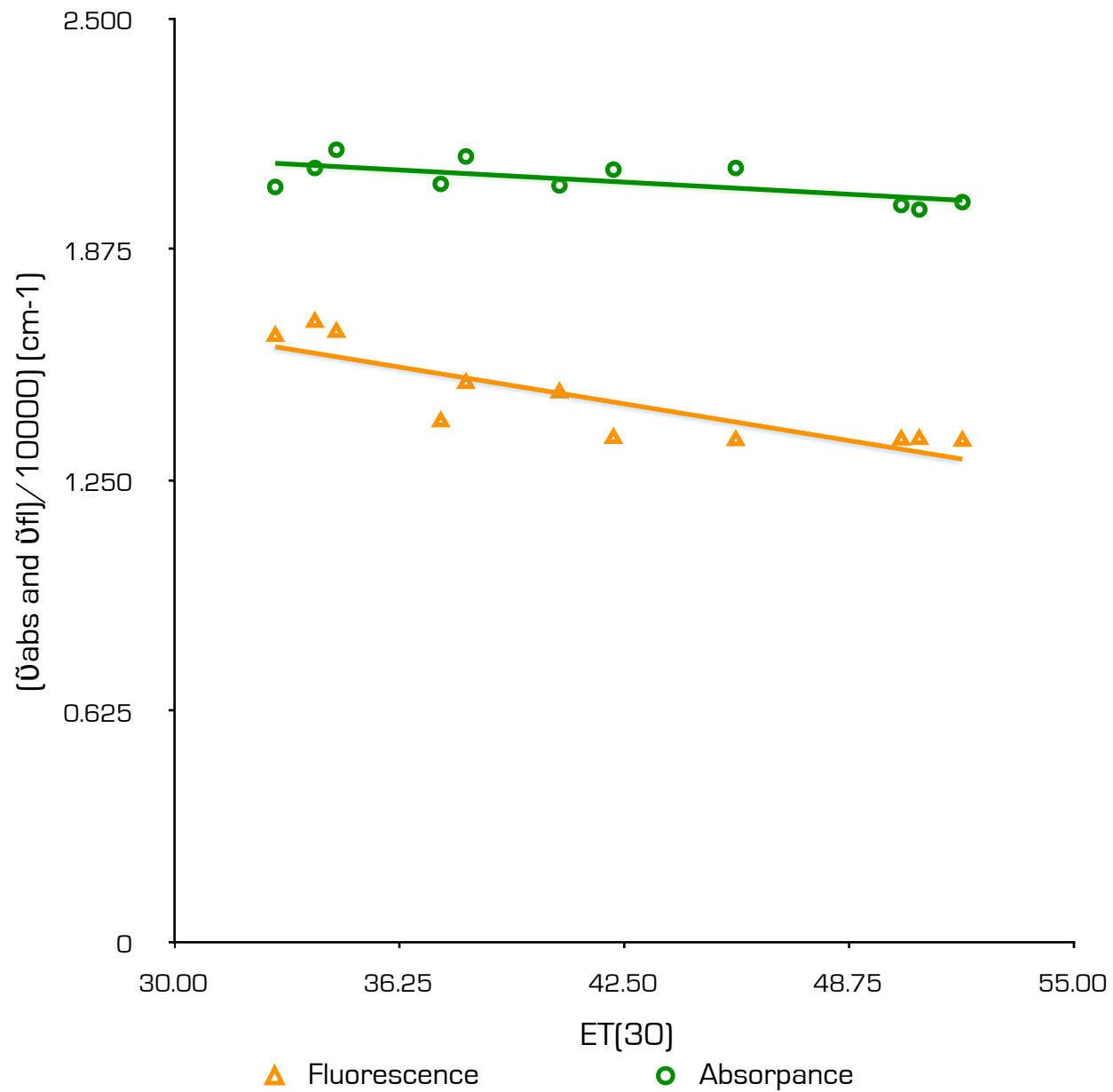


Figure 10: Plot of maximum absorption and fluorescence wavenumbers (divided by 10^4) versus the $E_T(30)$ scale in the various solvents

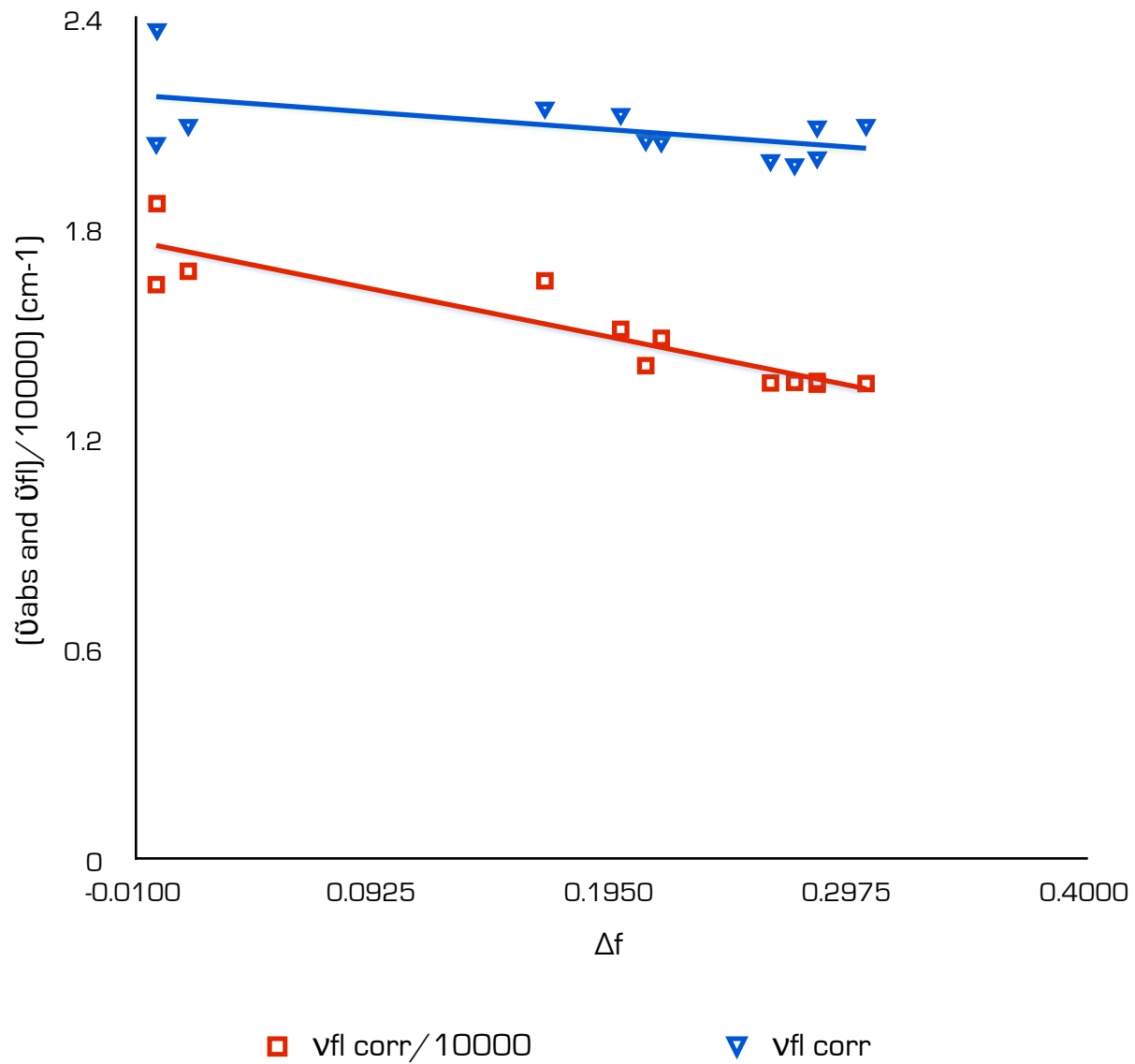


Figure 11: Plot of maximum absorption and fluorescence wavenumbers (divided by 10^4) versus the Δf scale in the various solvents

The quantum yield (Φ_f) was plotted against the fluorescence wavenumbers ($\tilde{\nu}_{fl}$) in figure 12. The figure shows a bell-like curve of the solvents in decreasing polarity. The quantum yield increases with polarity until it reaches solvents of moderate polarity, after which the quantum yields begin to fall again. This is due to a competition between intersystem crossing and internal conversion.

This phenomenon is determined by El Sayed's rule, which states that the rate of intersystem crossing is faster between two states of different orbital configurations when the S_1 state is higher in energy than the T_2 state. However, as polarity increases, the $T_2(n,\pi^*)$ state increases, which causes a decrease in the rate of intersystem crossing. The rate of intersystem crossing decreases with polarity, while the rate of internal conversion increases exponentially. Since Φ_f is given by the equation:

$$\Phi_f = \frac{k_f}{k_f + k_{nr}} \quad \text{Eq. 4}$$

$$k_{nr} = k_{ic} + k_{isc}$$

Where k_f is the first order radiative rate of decay, k_{nr} is the first order rate of non-radiative decay, k_{ic} is the rate of internal conversion, and k_{isc} is the rate of intersystem crossing. Therefore as k_{isc} decreases with polarity, the quantum yield increases. However since k_{ic} increases exponentially with polarity, it becomes the dominant factor, and quantum yield eventually decreases.

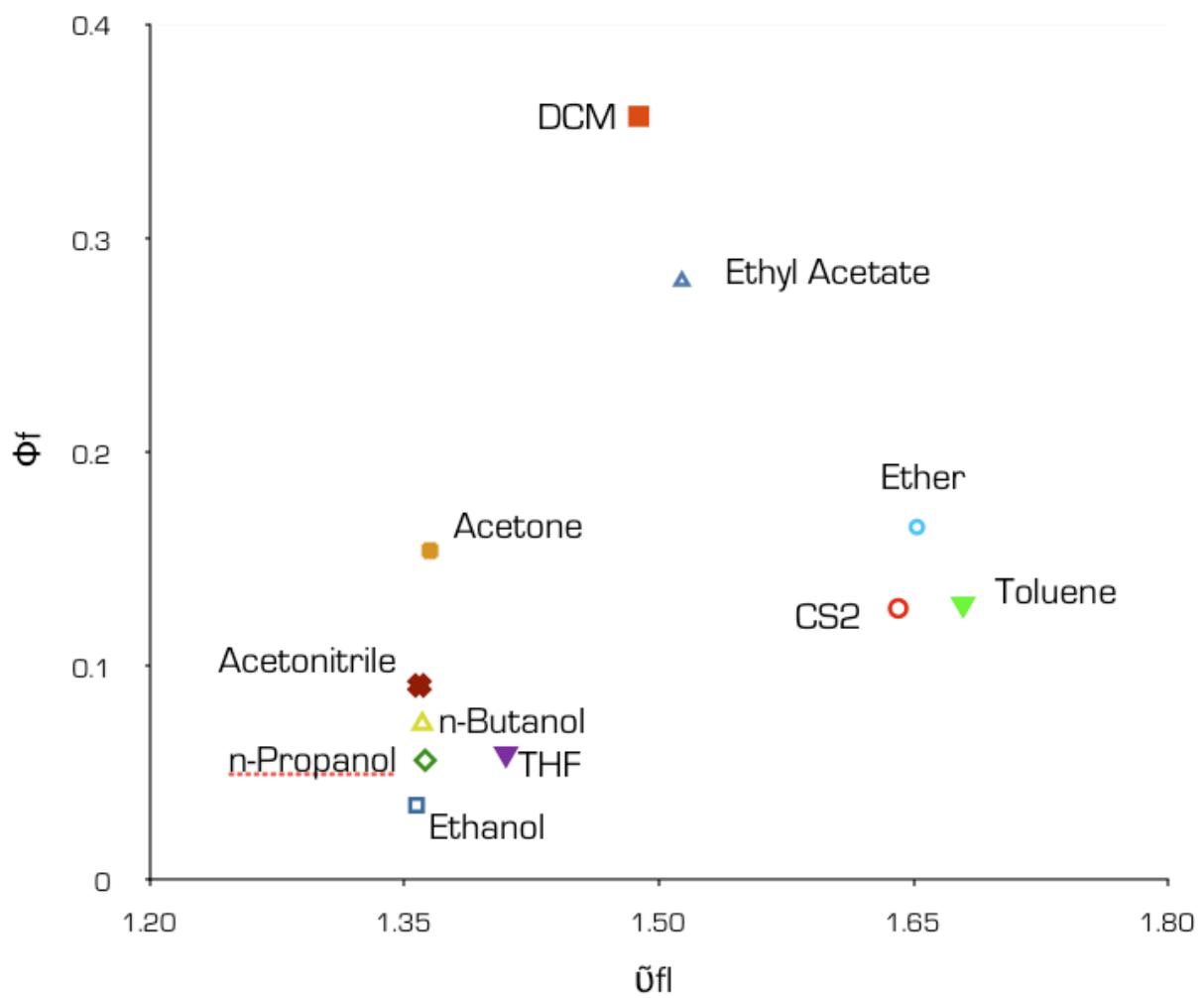


Figure 12: Plot of fluorescence quantum yield (Φ_f) versus \bar{n}_{fl} of ASBZ2 in solvents of varying polarities.⁷

The $\Delta\tilde{\nu}$ was plotted against Δf to give the Lippert-Mataga plot (Figure 13). The Lippert-Mataga Plot creates a linear relationship between the Stoke's Shift ($\Delta\tilde{\nu}$) and Δf . The equation provided by the trend line allows the calculation of the excited gas phase dipole moment. The equation ($y=mx+b$) for the line correlates to the equation⁸:

$$\Delta\nu = \frac{2\Delta\mu^2}{hca^3} \Delta f + \Delta\nu_0 \quad \text{Eq. 5}$$

$$\Delta\mu = \mu_e - \mu_g$$

Where h equals Planck's Constant ($6.626 \times 10^{-34} \text{ J}\cdot\text{s}$), c equals the speed of light in a vacuum ($2.998 \times 10^8 \text{ m/s}$), a is the Onsager cavity radius (calculated to be 6.0 \AA), and $\Delta\mu$ is the change in dipole moment. The ground state dipole moment (μ_g) and the Onsager cavity radius were calculated using Gaussian 3. μ_g was calculated to be 6.82 D , while $\Delta\mu$ was found to be 14.54 D , and μ_e was calculated to be 21.36 D . The large increase in dipole moment is due to charge transfer and the asymmetry of the molecule.

Lippert-Mataga Plot

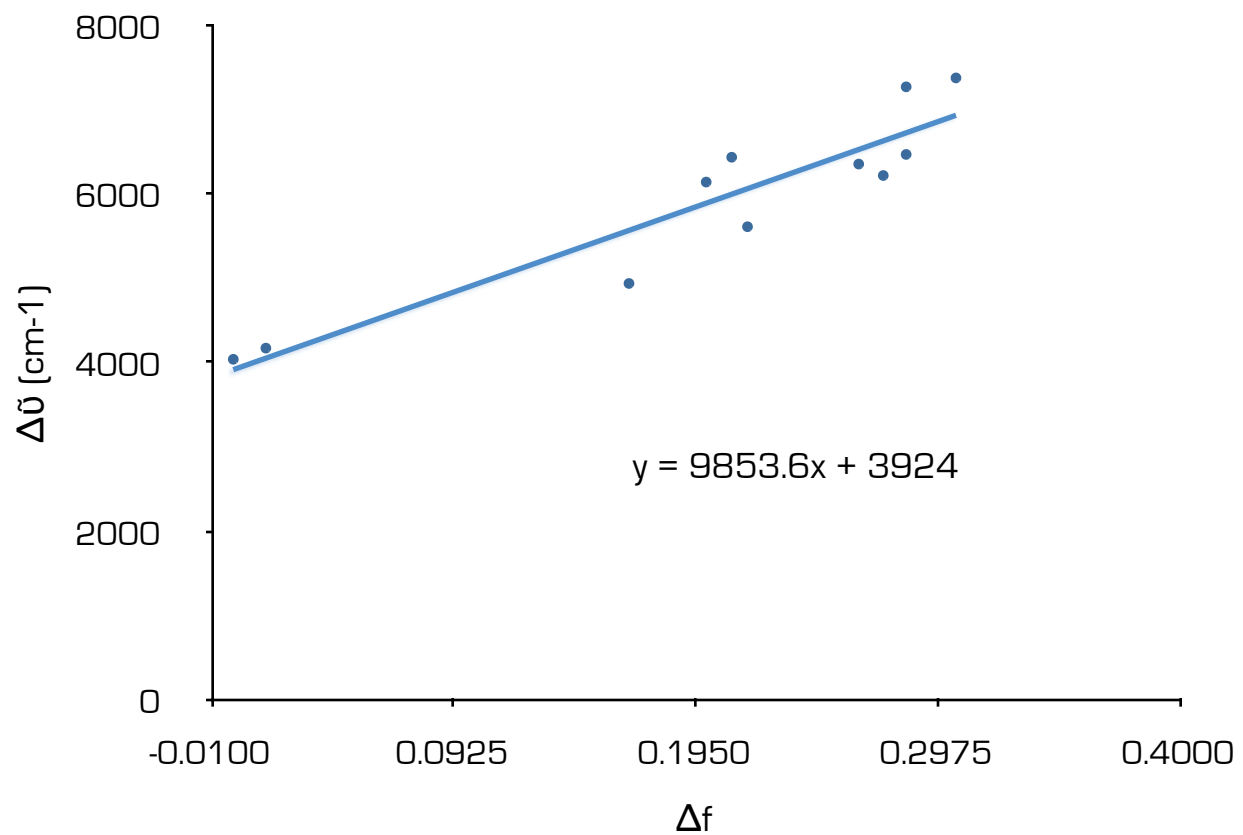


Figure 13: Lippert-Mataga Plot of Stoke's Shift ($\Delta\bar{\nu}$) versus Δf of compound II in the various solvents

Quantum Chemistry Calculations

DFT B3LYP/6-31G(d) geometry optimization and TD-DFT spectral calculations were performed on ASBZ2. The computed S1 transition internal charge transfer is shown in figure 14. Calculations show that the S0→S1 transition occurs via an ICT (π,π^*) mechanism. The S0→S2 transition is predicted to be (n,π^*). Calculated dipole moments, wavelengths, and oscillator strengths (f) are given in Table 2. The oscillator strengths express the strength of the transitions.

Table 2: Molecular Orbital Calculations of ASBZ2

HOMO→LUMO S ₁ (CT, π,π^*)	$\mu_{\text{ground}} = 6.82 \text{ D}$ (B3LYP/6-31G(d))
$\lambda=479.0 \text{ nm}$, $f=1.44$	
HOMO -2→LUMO S ₂ (n,π^*)	$\Delta\mu = 14.54 \text{ D}$ (Lippert-Mataga Plot)
$\lambda=440.4 \text{ nm}$, $f=0.00$	$\mu_{\text{excited}} = 21.36 \text{ D}$

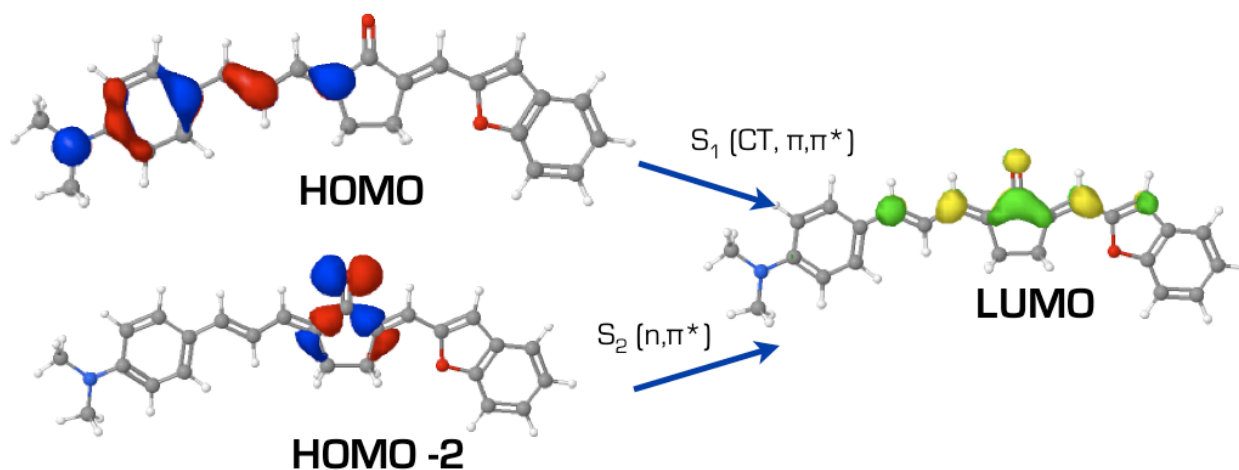


Figure 14: Computer molecular orbitals of ASBZ2

The molecular orbitals show a charge transfer from the amino group aromatic group to the carbonyl group for the HOMO→LUMO S_1 (CT, π,π^*) excitation. Since the compound is asymmetrically substituted, the dipole moment does not point directly at the carbonyl group, but is also pointed towards the benzofuran substituent.

Conclusions

The results of the spectroscopic and photophysical properties of ASBZ2 show that it exhibits solvatochromic properties in solvents of various polarities. The absorbance and emission show a correlation with regard to Δf and $E_T(30)$, and show that the Stoke's Shift for the compound increases with solvent polarity. The Lippert-Mataga plot showed a linear correlation between Stoke's Shift and the solvent polarity function. This confirms an electron charge transfer and a change in the electronic dipole moment from 6.82 D to 21.36 D. The fluorescent quantum yields also showed a change with solvent polarity consistent with El Sayed's Rule. Fluorescent lifetimes changed with solvent polarity, and the photophysical properties are attributed to the nonradiative rate of decay from the excited state S_1 . Finally, the quantum chemical calculations showed that the $S_0 \rightarrow S_1$ transition occurs via an ICT (π, π^*) mechanism, and the $S_0 \rightarrow S_2$ was predicted to be (n, π^*).

References

- ¹ Connors, R. E.; Ucak-Astarlioglu, M.G. *J. Phys. Chem. A* 2003, *107*, 7684
- ² "Fluorescent Multilayer Disc (FMD)" *BBC Home*. May 4th, 2001.
(<http://www.bbc.co.uk/dna/h2g2/A533143>)
- ³ Suppan, P.; Ghonheim, N. *Solvatochromism*; Royal Society of Chemistry: Cambridge, 1997.
- ⁴ Coolidge, A. S, James, H. M. and Present, R. D. *A study of the Franck-Condon Principle*; *Journal of Chemical Physics* 4: 193–211. 1936.
- ⁵ Strauss, C. R., et al., *Org. Lett.*, 2003, 5 (17), 3107-3110.
Strauss, C. R., et al., *Green Chem.*, 2006, 8, 1042-1050.
- ⁶ Rechthaler, K.; Kohler, G.; *Chem. Phys. Lett.* 1994, *189*, 99.
- ⁷ El-Sayed, M.A.; *J. Chem. Phys.* 1963, *38*, 2864
- ⁸ Nad, S.; Pal, H.; *J. Phys. Chem. A* 2001, *105*, 1097.

Appendices

Appendix A: Fluorescence Quantum Yield Sample Calculation

Connors

Quantum yield determination for ASBZ2 in Acetone Set 1
with red sensitive tube. Experiment 1

This QuickSheet demonstrates Mathcad's cspline and interp functions for connecting X-Y data.



Enter a matrix of X-Y data to be interpolated:

Enter spectral data for compound after converting to wavenumbers, multiplying intensity by lambda squared DO NOT normalize intensity. Insert data from Excel -right key, paste table.

data1 :=

1052.63	.46·10 ⁶
1030.49	.43·10 ⁶
21008.4	.36·10 ⁶
0986.36	...

Click on the Input Table above until you see the handles, and enlarge it to see the matrix data used in this example.

data1 := csort(data1, 0)

X := data1^{<0>}

Y := data1^{<1>}

Spline coefficients:

S1 := cspline(X, Y)

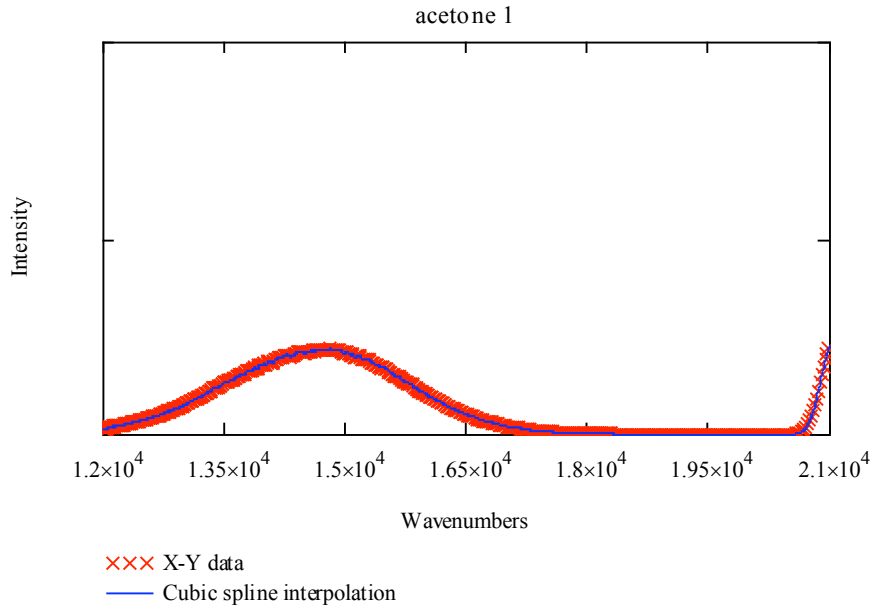
Fitting function:

fit(x) := interp(S1, X, Y, x)

Sample interpolated values:

$$\text{fit}(21000) = 2.317 \times 10^6$$

$$\text{fit}(18800) = 7.506 \times 10^3$$



Correction factors for LS50B with red sensitive tube

DATA Limits 12,500-22,200 Wavenumbers

corrdata :=

	0	1
0	12500	4.43
1	12550	...

xdata := csort(corrdata, 0)

A := corrdata^{<0>} B := corrdata^{<1>}

Spline coefficients:

S := cspline(A, B)

Fitting function:

Fitting function:

corrfit(x) := interp(S, A, B, x)

corrspec(x) := corrfi(x)·fit(x)

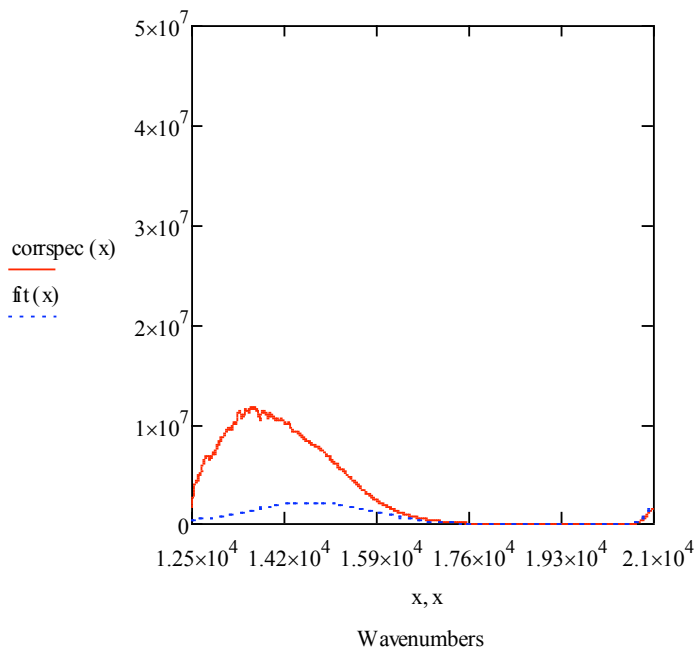
$\lambda := 12500 \dots 22200$

l =

1.25·10 ⁴
1.255·10 ⁴
1.26·10 ⁴
...

corrspec(l) =

1.751·10 ⁶
3.959·10 ⁶
4.566·10 ⁶
5.036·10 ⁶
...



$$\int_{12500}^{20600} \text{fit}(x) \, dx = 5.958 \times 10^9$$

$$\int_{12500}^{20600} \text{corrspec}(x) \, dx = 2.779 \times 10^{10}$$

Enter a matrix of X-Y data to be interpolated:

Enter spectral data for **standard** (fluorescein) after converting to wavenumbers, multiplying intensity by lambda squared DO NOT normalize intensities. Insert data from Excel -right key, paste table.

stdata :=

1052.63	1.11·10 ⁶
1030.49	.91·10 ⁶
1008.4	...

Click on the Input Table above until you see the handles, and enlarge it to see the matrix data used in this example.

```
stdata := csort(stdata, 0)
```

```
C := stdata <0>
```

```
D := stdata <1>
```

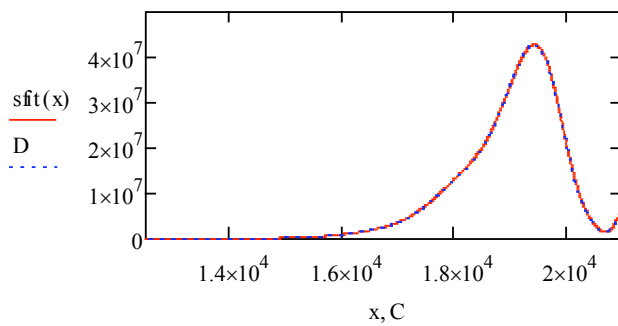
Spline coefficients:

```
S := cspline(C,D)
```

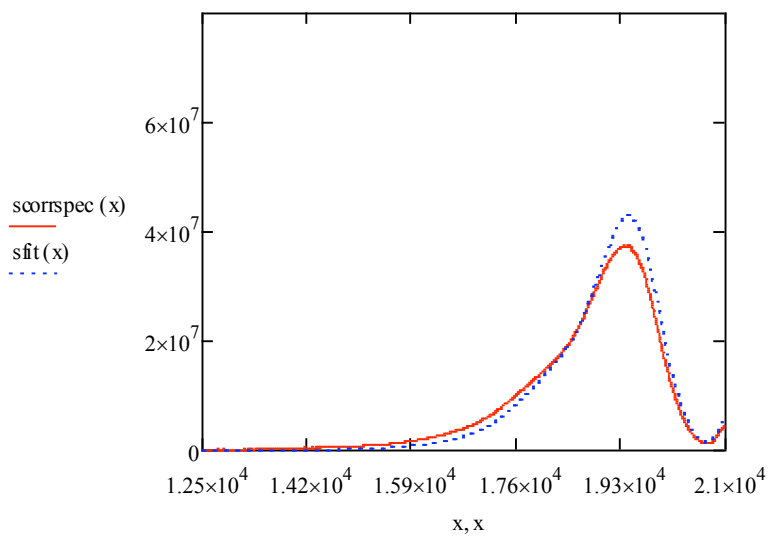
Fitting function:

```
sfit(x) := interp(S,C,D,x)
```

```
sfit(18000) = 1.328 × 107
```



```
scorspec(x) := corrfi(x) · (sfit(x))
```



Compound

Standard

$$\int_{12500}^{20600} \text{corrspec}(x) dx = 2.779 \times 10^{10}$$

$$\int_{12500}^{20600} \text{scorrsec}(x) dx = 7.29 \times 10^{10}$$

Area under corrected compound curve

Area under corrected standard curve

$$D_c := \int_{12500}^{20600} \text{corrsec}(x) dx$$

$$D_s := \int_{12500}^{20600} \text{scorrsec}(x) dx$$

$$D_c = 2.779 \times 10^{10}$$

$$D_s = 7.29 \times 10^{10}$$

Compound

Standard

Absorbance at (ex)
Index of refraction

$$A_c := 0.053$$

$$A_s := 0.0246$$

acetone

NaOH

$$n_c := 1.35$$

$$n_s := 1.41$$

quantum yield of
standard

$$QY_s := 0.9$$

$$QY_c := QY_s \cdot \left(\frac{A_s}{A_c} \right) \cdot \left(n_c \cdot \frac{n_c}{n_s \cdot n_s} \right) \cdot \left(\frac{D_c}{D_s} \right)$$

$$QY_c = 0.154$$

Appendix B: Fluorescence Lifetime Sample Calculations

Fluorescence Lifetime of ASBZ2 in Acetone

Analysis Function : Tue Apr 20 2010 at 14:40

***** one-to-four exponentials *****

***** Input Values *****

Decay curve : A1 478:671_acetone_200chan

IRF curve : A1 478:478_200chan

Start Time : 40.91

End Time : 50.11

Offset will be calculated

Shift will be calculated

Pre-exp. 1 : 1

Lifetime 1 : 1

***** Statistics *****

Job done after 6 iterations in 0.047 sec.

Fitted curve : FLD Fit (3)

Residuals : FLD Residuals (3)

Autocorrelation : FLD Autocorrelation (3)

Deconvolved Fit : FLD Deconvoluted (3)

Chi2 : 2.15

Durbin Watson : 1.905

Z : -0.03869

Pre-exp. 1 : 1.759 ± 1.652e-002 (100 ± 0.9395%)

Lifetime 1 : 0.7523 ± 8.135e-003

F1 : 1

Tau-av1 : 0.7523

Tau-av2 : 0.7523

Offset : -16.7

Shift : 0.3653

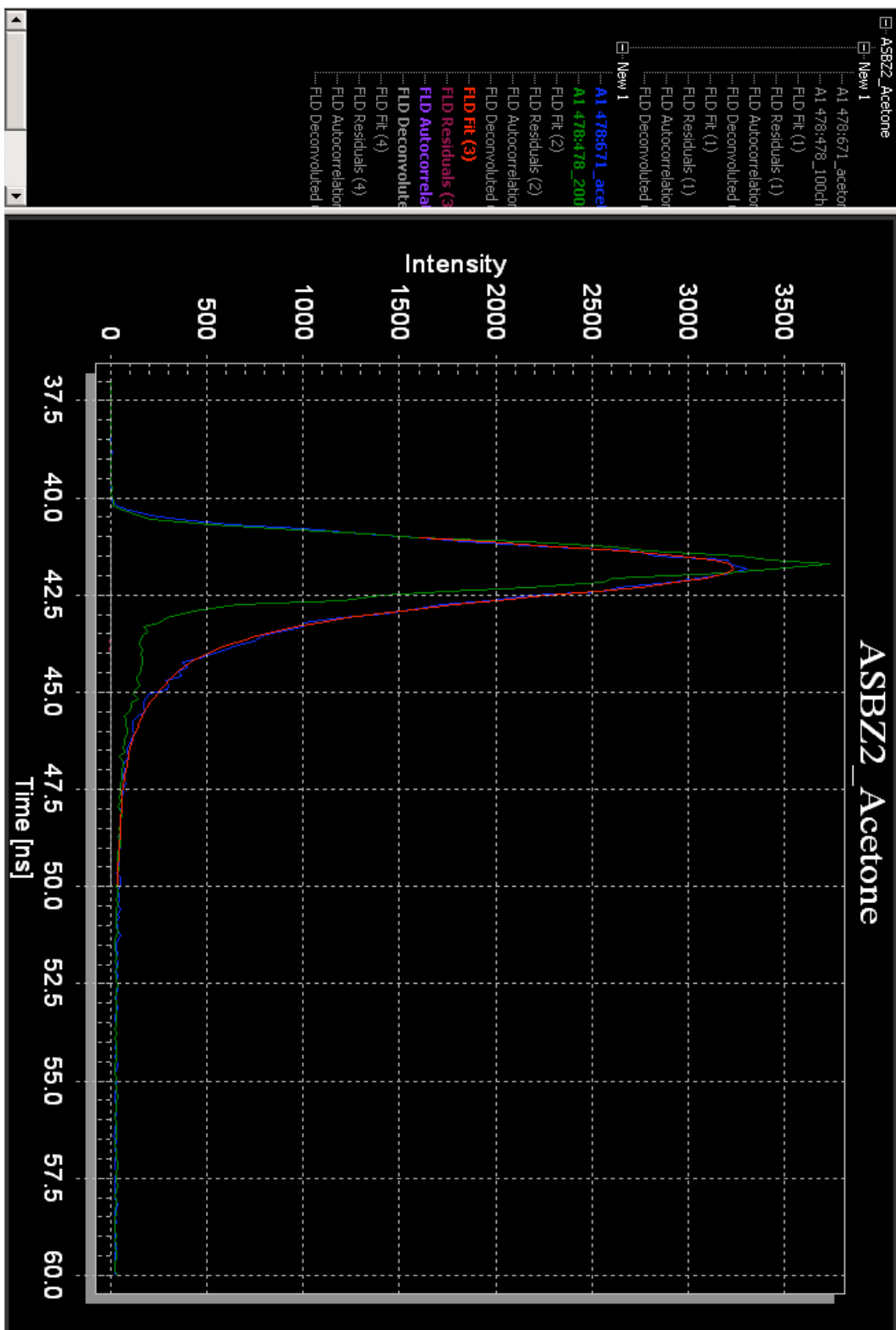


Figure 15: Fluorescence lifetime of ASBZ2 in acetone

